Available online at www.sciencedirect.com

ScienceDirect

IFAC PapersOnline CONFERENCE PAPER ARCHIVE

IFAC PapersOnLine 54-1 (2021) 1218–1223

Thermographic Indicators for the State Assessment of Rolling Bearings

Sebastian Roldan * **David Sanchez-Londono** *
Giacomo Barbieri *

* *Department of Mechanical Engineering, Universidad de los Andes, Bogotá (Colombia) (e.mail: {s.roldan10,d.sanchezl,g.barbieri}@uniandes.edu.co).*

Abstract: Within Prognostics and Health Management (PHM), State Assessment (SA) consists in the classification of the health state of a physical asset starting from the processing of signals acquired by selected sensors. Nowadays, Infrared Thermography (IRT) is successfully utilized with this purpose in different domains. However, the literature lacks of studies concerning the use of IRT for the SA of rolling bearings. In response to this issue, this work analyzes the potential that indicators obtained with passive thermography may have for classifying the severity of failures in the outer-race of rolling bearings. With this purpose, different single point defects were generated in the bearing outer-race with electrical discharge machining. Then, thermal images were acquired during the operation of the bearings, and indicators of the transient and steady-state behavior were calculated for the classification of the different health states. Four indicators presented a monotonic tendency with respect to the dimension of the defect, resulting promising for the SA of rolling bearings. Given the effectiveness that IRT has in other domains, we hope that this study may impulse the research in PHM of rolling bearings through IRT.

Keywords: Prognostics and Health Management, Fault Diagnosis Assessment, State Assessment, Infrared Thermography, Passive Thermography, Rolling Bearings, Outer-Race.

1. INTRODUCTION

Current maintenance strategies have progressed from breakdown maintenance to preventive and then to prognostics and health management (Martin, 1994). *Breakdown Maintenance* is the earliest form of maintenance, where no actions are taken to maintain the equipment until it breaks and consequently needs a repair or replacement. In the 1950s, *Preventive Maintenance* strategies were introduced and require maintenance on a time (or usage) interval regardless of the health condition of the physical asset. Later, *Prognostics and Health Management* (PHM, also known as Predictive Maintenance) emerged and is defined as a condition-driven preventive maintenance program divided into three main activities (Li et al., 2020): fault diagnosis assessment, prognostic assessment, and health management. *Fault Diagnosis Assessment* (FDA) deals with fault detection, isolation and identification (Jardine et al., 2006). Furthermore, FDA includes the *State Assessment* (SA) activity for classifying the severity of failures or the health state of the physical asset – in case the failure has not occurred yet.

Several techniques can be utilized for the SA of physical assets (Mobley, 2002), such as vibration and current monitoring, infrared thermography, tribology and ultrasonic amongst others. With respect to thermocouples and resistance temperature, *Infrared Thermography* (IRT) is a non-contact and non-invasive tool that provides the temperature distribution of a measured surface as a thermal image (Wang and Gao, 2006). IRT is being utilized as a condition monitoring technique in civil structures, electrical installations, machineries and equipment, material deformation under various loading conditions, corrosion damages and welding processes amongst others (Bagavathiappan et al., 2013). However, with regard to the PHM of rotating machinery, its use has been more limited (Lopez-Perez and Antonino-Daviu, 2017). In spite of this fact, the potential of IRT – together with the progressive decrease in the price of infrared cameras and the increase in their resolution (Hellier, 2001) – makes this tool an interesting option for condition monitoring.

IRT can be broadly classified into two major categories, viz. passive and active (Maldague, 2001). In *passive thermography*, the temperature of the object under investigation is recorded without any external heat stimulation, as the object itself acts as a source of heat. On the other hand, external heat stimulation is essential for *active thermography* experiments. Passive thermography is generally utilized for PHM of rotating machinery since the defective regions appear as hot-spots, and significant temperature difference exists between defect and defect-free regions (Osornio-Rios et al., 2018). Therefore, passive thermography has been adopted within this work.

The *SA of rolling bearings* is paramount for improving the reliability and performance of rotating machinery, since bearing failures are among the most frequent causes of breakdowns. For instance, bearing failures can account for up to 44% of the total number of faults in the case of large induction motors (Zhang et al., 2010). Recent literature reviews concerning the SA of rolling bearings

10.1016/j.ifacol.2021.08.208

are presented in Cerrada et al. (2018), and El-Thalji and Jantunen (2015). Physics-based and data-driven models are illustrated analyzing their effectiveness in identifying degradation patterns with regards to health conditions. Techniques and methods based on vibration, acoustic emission, current and voltage signals are discussed within these literature reviews. However, approaches based on IRT are not considered.

Several works can be found concerning the application of *IRT* for the *FDA of rolling bearings*. Lopez-Perez and Antonino-Daviu (2017) illustrated the effectiveness of IRT for the detection of a wide range of failures in induction motors. Through an infrared camera, they inspected a sample of motors operating in a petrochemical plant. Anomalies were identified by comparing the relative temperature between faulty and healthy motors under similar operative conditions. The studied anomalies had different origins, and included deficient bearing lubrication and damaged bearings. Kim et al. (2010) demonstrated the capability of IRT for the detection of defects on the outer-race of rolling bearings. They compared the temperature evolution of faulty and healthy bearings at different operative conditions; i.e. angular velocities. After a transient behavior, faulty bearings always reached higher steady-state temperatures than the healthy ones. Similar results were obtained by Nunez et al. (2016) and Huo et al. (2017). Finally, Singh and Naikan (2017) proposed two thermal profile indicators for induction motors to differentiate in between inter-turn and cooling system failures.

It can be noticed that the papers presented above only deal with fault detection and identification, but do not consider the SA of rolling bearings. The only work related to the investigation of *IRT* for the *SA of rolling bearings* can be found in Mazioud et al. (2008). Here, authors analyzed the spalling defect on the outer-race of rolling bearings. Through experiments, they demonstrated that the temperature on the bearing surface was proportional to the vibratory level generated by the progressive appearance of the defect. Therefore, they showed that IRT seems viable for the SA of rolling bearings, even if they did not attempt to classify the severity of the failures.

Given the above, this work analyzes different indicators for the SA of rolling bearings through passive thermography. The paper is structured as follow: the utilized experimental methodology is illustrated in section 2. Section 3 shows the indicators evaluated for the classification of the health state. Obtained results are discussed in section 4 and finally, section 5 presents the conclusions and sets the directions for future work.

2. EXPERIMENTAL METHODOLOGY

The adopted *experimental methodology* is represented in Figure 1 and is illustrated in this section. In particular, section 2.1 presents the utilized test bench and the planned experiment. Section 2.2 shows the technical decisions and the environmental conditions taken into account for the acquisition of the bearing surface temperature through an infrared camera. Section 2.3 discusses a preliminary experiment implemented for defining the experiment duration and the sampling frequency. Finally, Section 2.4 describes the data collection process and the format of the obtained images.

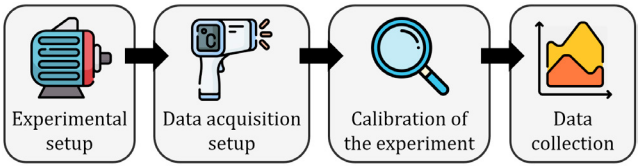

Fig. 1. Adopted experimental methodology

2.1 Experimental setup

The *test bench* shown in Figure 2 was utilized for simulating the operation of faulty and healthy bearings. This test bench consists of an induction motor, a flywheel, and three ball bearings. It allows the simulation of bearing failures, shaft misalignment, and unbalanced loads. Moreover, different operative conditions can be run by changing the frequency supplied to the motor. However, only one operative condition has been investigated within this work, being a first research on the topic.

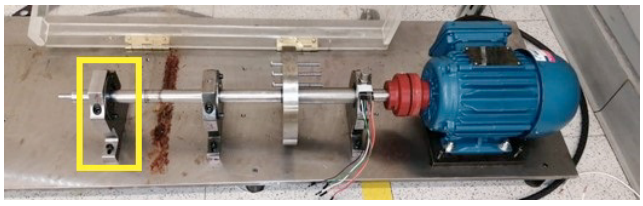

Fig. 2. Induction motor test bench utilized for the simulation of bearing failures. The tested bearing is indicated with a yellow rectangle

To evaluate indicators for the SA of rolling bearings, an approach similar to the one adopted in Barbieri et al. (2020) was utilized. In that work, authors generated discrete unbalanced conditions by placing screws, nuts and washers on the flywheel of the test bench. Then, vibration signals were acquired during the system operation, and different indicators were evaluated for the classification of the severity of the unbalance. In this work – with the objective to produce *discrete faulty conditions* in 6204-2RSH ball bearings [1] – different single point defects were generated in the bearing outer-race with electrical discharge machining. A notch was seeded on each bearing for the definition of three severity levels. Each level had an approximate depth of 0.3mm, and a width of 0.233mm (severity 1), 0.349mm (severity 2), and 0.549mm (severity 3); see Figure 3. Whereas, the length of the notch was equal to the depth of the outer-race.

During each experimental run, the tested bearing was mounted in the configuration shown in Figure 2. Then, the motor was run and thermal images were taken with an infrared camera.

2.2 Data acquisition setup

The factors that affect the accuracy of IRT measurements can be categorized as technical and environmental

[1] https://www.skf.com/group/products/rolling-bearings/ball-bearings/deep-groove-ball-bearings/productid-6204-2RSH

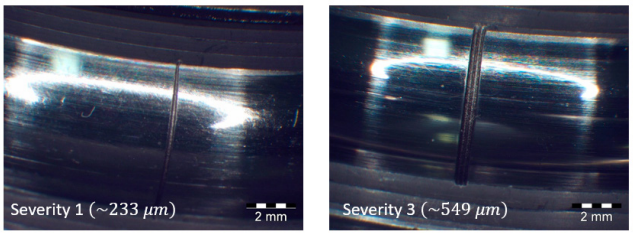

Fig. 3. Single point defects seeded on the bearing outer-race for the generation of different severity levels. Severity 1 and 3 are illustrated using a stereo microscope

conditions (Jadin and Taib, 2012). For *technical factors*, the necessary information concerns the utilized infrared camera, the emissivity of the equipment under inspection, its operative condition, the distance of the object being inspected, and the Region of Interest (ROI) within the obtained image. The *environmental factors* depend on the type of assessment. For instance, environmental temperature is generally sufficient for indoor measurements (Leemans et al., 2011), while humidity, solar radiation and wind direction are important factors within outdoor measurements (Balaras and Argiriou, 2002).

The setup implemented for the data acquisition is shown in Figure 4. Its technical and environmental conditions are next illustrated:

- *Technical*:
  - *Camera*: Fluke Ti45FT IR FlexCam [2]
  - *Emissivity*: a value of 0.95 was set considering that the bearing case is made of SAE 1010 oxidised carbon steel [3]
  - *Operative condition*: only one operative condition was investigated within the experiment. The induction motor was supplied with 60Hz three-phase electric power, running approximately at 1710rpm
  - *Distance*: the camera was located at a distance of 500mm from the bearing
  - *Region of interest*: the utilized ROI is illustrated in Figure 4. A square box of 48 × 48 pixels was selected, making sure that the tested bearing was included on it
- *Environmental*: since the experiment was performed indoor, only the environmental temperature was measured

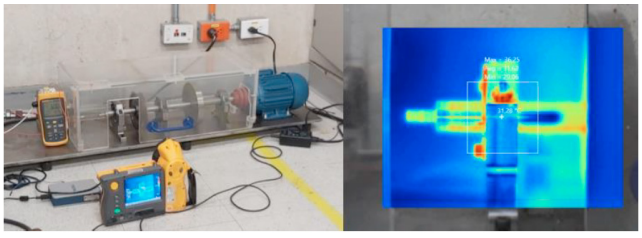

Fig. 4. Experimental setup including the location of the camera, and the selected ROI; i.e. the square box on the right-hand side image

[2] https://www.fluke.com/en/product/thermal-cameras/ti45ft
[3] https://www.calex.co.uk/site/wp-content/uploads/2015/07/emissivity-tables.pdf

2.3 Calibration of the experiment

In the experiment, the system started from rest and the temperature of the tested bearing corresponded to the environmental one. Then, the system was run and a transient behavior occurred before reaching the steady-state temperature. Therefore, it was important to estimate the minimum duration that had to be set for the experiment.

A *duration test* was performed with this purpose. The system was run for 220 minutes (3:40 hours) with a faulty bearing with severity 3; i.e. maximum severity level. Figure 5 illustrates the evolution of the maximum bearing temperature over time. Then, the temperature behavior was approximated using the exponential model described in Section 3.2, obtaining the following mathematical expression:

$$T_{max}(t) = \frac{0.8523}{0.02301} - 13.47e^{-0.02301t} \quad (1)$$

In systems with exponential behavior, it is possible to quantify a time constant τ to estimate the time necessary to reach a given percentage of the system response (Rowell and Wormley, 1996). The value of τ corresponds to the inverse of the time coefficient within the exponential term; i.e. 0.02301 in equation (1). Then, the percentage of the system response (y_s) can be calculated with the following expression:

$$y_s(t) = 1 - e^{-t/\tau} \quad (2)$$

For the behavior represented in Figure 5, a τ of 43.46 minutes was computed. Then, a percentage of 93.7% was obtained by considering a duration of 120 minutes. Therefore, this value was the duration set for the experiment.

With respect to the *sampling frequency*, low frequencies are utilized in IRT experiments since the steady-state behavior is generally the only analyzed behavior. For instance, an image is taken each 10 minutes in Marinescu et al. (2017), and each 5 minutes in Jeffali et al. (2015). However, we decided to take one image each 2 minutes. This value corresponds to more than 20 times the system time constant, enabling the acquisition of the transient behavior.

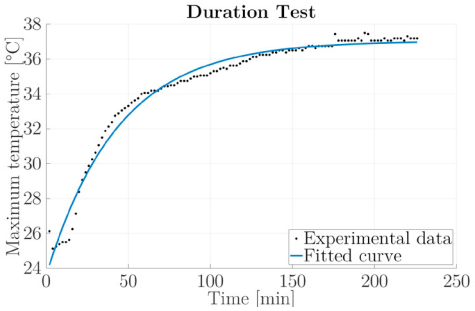

Fig. 5. Bearing maximum temperature evolution during the duration test, and its exponential approximation. The mean squared error between the experimental and the estimated values is 0.2234°C

2.4 Data collection

Given the emissivity, the environmental temperature and the ROI, the camera acquired thermal images using the

selected sampling frequency. Then, the images were converted into *temperature profile matrices* in which a temperature value is associated to each pixel (Jeffali et al., 2019). A 48×48 matrix was obtained from each image, in which each element of the matrix corresponded to the temperature of the considered pixel; see Figure 6. This conversion facilitated the data processing, since real-valued matrices were analyzed in place of RGB images.

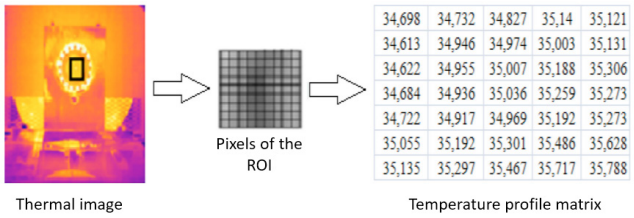

Fig. 6. Conversion of a thermal image into a temperature profile matrix. The representation has been adopted from Jeffali et al. (2019)

3. THERMOGRAPHIC INDICATORS OF ROTATING MACHINERY

In this section, thermographic indicators commonly utilized for the analysis of the steady-state behavior of rotating machinery are presented (sec. 3.1). Furthermore, indicators relative to the transient behavior are introduced in section 3.2, by considering the heat transfer phenomena involved during the bearing operation.

3.1 Steady-state behavior

The thermal condition of rotating machinery can be identified using two ΔT methods (Lopez-Perez and Antonino-Daviu, 2017). These ΔT methods are utilized by the International Electrical Testing Association (NETA) to recommend maintenance actions for electrical systems and rotating equipment (NETA, 2008). The first method is known as *quantitative criteria* and consists in calculating the relative temperature between the maximum temperature of the equipment and the environmental one. The second method is known as *qualitative criteria* and consists in calculating the relative temperature between the maximum temperature of the equipment and the one of a healthy equipment operating under similar conditions (Jadin and Taib, 2012). According to the ΔT methods, the quantitative criteria for rolling bearings can be computed as:

$$\Delta T_{quant} = T_m - T_a \tag{3}$$

where T_m is the maximum temperature value of the tested bearing, and T_a is the ambient temperature. Whereas, the qualitative criteria for rolling bearings can be computed as:

$$\Delta T_{qual} = T_m - T_h \tag{4}$$

where T_m is the maximum temperature value of the tested bearing, and T_h is the maximum temperature value of a healthy bearing operating under similar conditions.

Further indicators can be identified by considering all the pixels of the ROI, and not only the maximum temperature. The temperature profile matrix $[T]_{m\times n}$ – corresponding to the captured thermal image (see Fig. 6) – can be converted into a column matrix $[Tx]_{(m*n)\times 1}$ to calculate its *mean* and *standard deviation*:

$$Tx_{mean} = \frac{\sum_k [Tx]_k}{m*n} \tag{5}$$

$$Tx_{std} = \sqrt{\frac{1}{m*n-1} * \sum_k ([Tx]_k - Tx_{mean})^2} \tag{6}$$

On the other hand, given $[Tt]$ the vector containing the temperature of the pixels above an established *temperature threshold*, the following indicators can be computed:

$$Tt_{\%} = \frac{length([Tt])}{m*n} \tag{7}$$

$$(Tt_{\%})_{fh} = (Tt_{\%})_f - (Tt_{\%})_h \tag{8}$$

where $Tt_{\%}$ is the percentage of pixels with temperature above the selected threshold; see Figure 7. $(Tt_{\%})_f$ is the percentage for the analyzed faulty bearing, and $(Tt_{\%})_h$ the percentage for a healthy bearing.

29.8	32.8	31.2	30.3
29.7	31.5	30.6	29.4
28.1	29.6	30.1	28.8
26.8	27.9	29.2	27.6

Threshold: 30°C
■ = Above threshold
□ = Below threshold
$Tt_{\%} = \frac{6}{4*4} = 37.5\%$

Fig. 7. Example for the calculation of $Tt_{\%}$

The presented 'pixel-based' indicators have been proposed in Singh and Naikan (2017) to differentiate in between inter-turn and cooling system failures of induction motors.

3.2 Transient behavior

It can be noticed that the aforementioned indicators only deal with the steady-state behavior of the equipment. Therefore, we decided to include the calculation of additional indicators for representing the transient behavior. In this section, an exponential model that approximates the behavior of the temperature is first identified. Then, the model is utilized for defining thermographic indicators relative to the transient behavior.

During the operation of a bearing, energy is supplied through conductive heat transfer – due to the friction in between the rotating elements of the bearing – and is output through convective heat transfer. Since the supplied energy comes from the mechanical work (e.g. shaft rotation, vibrations, etc.), the following equation can be utilized for modeling the *thermal behavior* of the bearing (Cengel et al., 2019):

$$c_p \dot{T}(t) = \dot{W} - hA(T(t) - T_a) \tag{9}$$

where c_p is the specific heat capacity of the system, $\dot{W}$ is the mechanical work, h is the convection heat transfer coefficient, A is the surface area where convection takes place, and T_a is the ambient temperature. Equation (9)

models a first order differential equation that can be analytically solved as:

$$T(t) = \frac{K_2}{K_1} - c_1 e^{-K_1 t} \quad \text{where } K_1 = \frac{hA}{c_p},\ K_2 = \frac{hAT_a + \dot{W}}{c_p} \tag{10}$$

The *exponential model* shown in equation (10) can be utilized for approximating the behavior of the temperature over time, and was adopted in section 2.3 for the identification of the experiment duration.

The parameters identified in equation (10) can be utilized for defining *indicators* relative to the transient behavior of the maximum temperature. It can be noticed that K_1 and K_2 are function of characteristic properties of the system, such as the convection heat transfer coefficient h and the specific heat capacity c_p. Furthermore, K_2 also depends on the system operative condition; i.e. the ambient temperature T_a and the supplied mechanical work $\dot{W}$. As illustrated in equation (11)-(12), the ratio between K_2 and K_1 represents the estimated value of the steady-state temperature, while c_1 indicates the estimated temperature difference between the initial temperature (i.e. T_a) and the steady-state one:

$$T(t \to \infty) = T_\infty = \frac{K_2}{K_1} \tag{11}$$

$$T(t = 0) = T_a = \frac{K_2}{K_1} - c_1 \to c_1 = T_\infty - T_a \tag{12}$$

The aforementioned considerations make K_1 and K_2 potential thermographic indicators for the transient behavior of rolling bearings. Whereas, c_1 represents an estimation of the ΔT_{quant} indicator (see equation (3)), and K_2/K_1 indicates the estimation of the steady-state temperature. It can be noticed that the information content of c_1 and K_2/K_1 has already been included within the steady-state indicators and will not be computed in section 4.

4. RESULTS AND DISCUSSION

In this section, the identified steady-state and transient indicators are computed to analyze their potential for the SA of rolling bearings. One healthy and three faulty bearings with different severity levels were tested following the setup and parameters defined in section 2. Then, the *indicators* presented in section 3 were calculated. The obtained results are synthesized in Table 1. In the table, H indicates the healthy bearing, while S a faulty bearing with its severity specified through an integer value. It must be noted that the percentage of pixels with temperature above a selected threshold (i.e. $Tt_{\%}$) is computed by assuming a threshold of $T_a + 10°C$. The value of $10°C$ is selected by considering that the NETA suggests to repair rotating equipment when this ΔT is reached with respect to the environmental temperature (NETA, 2008).

The results shown in Table 1 are analyzed through a *monotonic tendency metric*; viz. a 'good' indicator is expected to increase monotonically with the severity of the failure. Four of the identified indicators have a monotonic tendency with respect to the dimension of the defect, resulting promising for the SA of rolling bearings. However, possible *outliers* may be present since the experiment was repeated just once. Considering that the objective of the paper was to identify potential indicators, the statistical validation of the obtained results through different repetitions of the experiment is left as future work.

Finally, it is important to note that all the indicators were obtained starting from the *domain knowledge*. Even if only half of the identified indicators seems promising, we expect the results to improve with their statistical validation – due to the cancellation of the outliers. In fact, indicators obtained from the domain knowledge are generally useful for classifying the health state; see Barbieri et al. (2020).

Table 1. Steady-state and transient indicators

	H	S1	S2	S3	Monotonic tendency
ΔT_{quant}(°C)	15.07	15.40	15.80	20.00	Yes
ΔT_{qual}(°C)	0.00	-0.38	1.22	2.75	No
Tx_{mean}(°C)	31.84	32.30	32.50	32.96	Yes
Tx_{std}(°C)	1.55	1.64	1.84	2.36	Yes
$Tt_{\%}$	0.24	0.51	0.28	0.92	No
$(Tt_{\%})_{fh}$	0.00	0.27	0.04	0.68	No
K_1 (1/s)	0.04	0.04	0.04	0.05	No
K_2 (°C/s)	1.32	1.48	1.67	2.11	Yes

5. CONCLUSION AND FUTURE WORK

Considering the high percentage of faults caused by rolling bearings, the *State Assessment* of these components can bring several benefits in terms of reliability and performance of rotating machinery. Techniques and methods based on vibration, acoustic emission, current and voltage signals have been utilized for this task. However, approaches based on *Infrared Termography* have not been considered yet.

In this context, the objective of this research work was to explore the potential that *indicators* obtained with passive thermography may have for classifying the severity of failures in the outer-race of rolling bearings. With this purpose, different single point defects were generated in the bearing outer-race with electrical discharge machining, and thermal images were acquired during the operation of the bearings. Typical indicators relative to the *steady-state behavior* of rotating machinery were computed. Furthermore, indicators relative to the *transient behavior* were introduced by considering the heat transfer phenomena involved during the bearing operation. Four indicators presented a monotonic tendency with respect to the dimension of the defect, resulting promising for the SA of rolling bearings.

Notably, the proposed approach and indicators constitute preliminary concepts for certifying the ability of IRT to classify the health state of rolling bearings. Some *future works* identified are:

- *Experiment repetitions*: the objective of this research work was to define promising indicators for the SA of rolling bearings. Next, the proposed experiment should be repeated to statistically validate the obtained results

- *Operative condition*: since the heat generated within a bearing is proportional to the product of the bearing torque and the rotational speed (Hannon and Houpert, 2013), the classification of the health state should be a function not only of the steady-state and transient behavior, but also of the operative condition. Experiments at different operative conditions should be performed to quantify its influence in the SA of rolling bearings
- *Robustness to noise*: once evaluated the ability of IRT to classify the health state of rolling bearings for 'laboratory' conditions, the effects of different noises – typical of industrial workplaces – should be investigated; e.g. variations in environmental temperature, dust, light, and emissivity amonsts others.

REFERENCES

Bagavathiappan, S., Lahiri, B., Saravanan, T., Philip, J., and Jayakumar, T. (2013). Infrared thermography for condition monitoring–a review. *Infrared Physics & Technology*, 60, 35–55.

Balaras, C.A. and Argiriou, A. (2002). Infrared thermography for building diagnostics. *Energy and buildings*, 34(2), 171–183.

Barbieri, G., Sanchez-Londono, D., Cattaneo, L., Fumagalli, L., and Romero, D. (2020). A Case Study for Problem-based Learning Education in Fault Diagnosis Assessment. *IFAC-PapersOnline*.

Cengel, Y.A., Boles, M.A., and Kanoğlu, M. (2019). *Thermodynamics: An Engineering Approach*. McGraw-Hill Education, 9th edition.

Cerrada, M., Sánchez, R.V., Li, C., Pacheco, F., Cabrera, D., de Oliveira, J.V., and Vásquez, R.E. (2018). A review on data-driven fault severity assessment in rolling bearings. *Mechanical Systems and Signal Processing*, 99, 169–196.

El-Thalji, I. and Jantunen, E. (2015). A summary of fault modelling and predictive health monitoring of rolling element bearings. *Mechanical systems and signal processing*, 60, 252–272.

Hannon, W. and Houpert, L. (2013). Rolling bearing heat transfer and temperature. *Encyclopedia of Tribology*, 2831–2839.

Hellier, C. (2001). *Handbook of nondestructive evaluation*. McGraw-Hill Professional.

Huo, Z., Zhang, Y., Sath, R., and Shu, L. (2017). Self-adaptive fault diagnosis of roller bearings using infrared thermal images. In *43rd Annual Conference of the IEEE Industrial Electronics Society (IECON)*, 6113–6118.

Jadin, M.S. and Taib, S. (2012). Recent progress in diagnosing the reliability of electrical equipment by using infrared thermography. *Infrared Physics & Technology*, 55(4), 236–245.

Jardine, A.K., Lin, D., and Banjevic, D. (2006). A review on machinery diagnostics and prognostics implementing condition-based maintenance. *Mechanical systems and signal processing*, 20(7), 1483–1510.

Jeffali, F., Kihel, B., Nougaoui, A., and Delaunois, F. (2015). Monitoring and diagnostic misalignment of asynchronous machines by infrared thermography. *J. Mater. Environ. Sci*, 6(4), 1192–1199.

Jeffali, F., Ouariach, A., El Kihel, B., and Nougaoui, A. (2019). Diagnosis of three-phase induction motor and the impact on the kinematic chain using non-destructive technique of infrared thermography. *Infrared Physics & Technology*, 102, 102970.

Kim, D., Yun, H., Yang, S., Kim, W., and Hong, D. (2010). Fault diagnosis of ball bearings within rotational machines using the infrared thermography method. *Journal of Korean Society of Nondestructive Testing*, 30(6), 558–563.

Leemans, V., Destain, M.F., Kilundu, B., and Dehombreux, P. (2011). Evaluation of the performance of infrared thermography for on-line condition monitoring of rotating machines. *Engineering*, (3), 1030–1039.

Li, R., Verhagen, W.J., and Curran, R. (2020). A systematic methodology for Prognostic and Health Management system architecture definition. *Reliability Engineering and System Safety*, 193.

Lopez-Perez, D. and Antonino-Daviu, J. (2017). Application of infrared thermography to failure detection in industrial induction motors: case stories. *IEEE Transactions on Industry Applications*, 53(3), 1901–1908.

Maldague, X. (2001). *Theory and practice of infrared technology for nondestructive testing*. Wiley.

Marinescu, A.D., Cristescu, C., Popescu, T.C., and Safta, C.A. (2017). Assessing the opportunity to use the infrared thermography method for predictive maintenance of hydrostatic pumps. In *2017 International Conference on Energy and Environment (CIEM)*, 270–274. IEEE.

Martin, K. (1994). A review by discussion of condition monitoring and fault diagnosis in machine tools. *International Journal of Machine Tools and Manufacture*, 34(4), 527–551.

Mazioud, A., Ibos, L., Khlaifi, A., and Durastanti, J. (2008). Detection of rolling bearing degradation using infrared thermography. In *Proceeding of the 9th International Conference on Quanitative Infrared Thermography*.

Mobley, R.K. (2002). *An introduction to predictive maintenance*. Elsevier.

NETA (2008). Standard for infrared inspection of electrical systems & rotating equipment. Technical report, International Electrical Testing Association.

Nunez, J., Velazquez, L., Hernandez, L., Troncoso, R., and Osornio-Rios, R. (2016). Low-cost thermographic analysis for bearing fault detection on induction motors. *Journal of Scientific and Industrial Research*, 75(7), 412–415.

Osornio-Rios, R.A., Antonino-Daviu, J.A., and de Jesus Romero-Troncoso, R. (2018). Recent industrial applications of infrared thermography: A review. *IEEE Transactions on Industrial Informatics*, 15(2), 615–625.

Rowell, D. and Wormley, D.N. (1996). *System Dynamics: An Introduction*. Pearson, 1st edition.

Singh, G. and Naikan, V. (2017). Infrared thermography based diagnosis of inter-turn fault and cooling system failure in three phase induction motor. *Infrared Physics & Technology*, 87, 134–138.

Wang, L. and Gao, R.X. (2006). *Condition monitoring and control for intelligent manufacturing*. Springer Science & Business Media.

Zhang, P., Du, Y., Habetler, T.G., and Lu, B. (2010). A survey of condition monitoring and protection methods for medium-voltage induction motors. *IEEE Transactions on Industry Applications*, 47(1), 34–46.